T2R2 東京科学大学 リサーチリポジトリ
Science Tokyo Research Repository

論文 / 著書情報
Article / Book Information

Title	DEVELOPMENT OF BENDING-SHEAR MODEL FOR SIMPLIFIED ANALYSIS OF SUPER-TALL BUILDINGS
Authors	K. Kasai, K. Watai, S. Maeda, D. Sato, Y. Suzuki
Pub. date	2020, 9
Citation	2020 17WCEE Proceedings

Powered by T2R2 (Science Tokyo Research Repository)

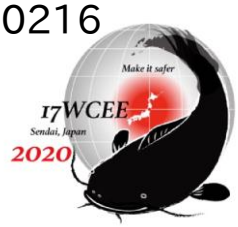

17th World Conference on Earthquake Engineering, 17WCEE
Sendai, Japan - September 13th to 18th 2020

DEVELOPMENT OF BENDING-SHEAR MODEL FOR SIMPLIFIED ANALYSIS OF SUPER-TALL BUILDINGS

K. Kasai[(1)], K. Watai[(2)] , S. Maeda[(3)], D. Sato[(4)], Y. Suzuki[(5)]

[(1)] *Specially Appointed Professor, Tokyo Institute of Technology, kasai.k.ac@m.titecha.c.jp*
[(2)] *Specially Appointed Assistant Professor, Tokyo Institute of Technology, watai.k.aa@m.titech.ac.jp*
[(3)] *Takenaka Corporation, maeda.shuusaku@takenaka.co.jp*
[(4)] *Associate Professor, Tokyo Institute of Technology, sato.d.aa@m.titech.ac.jp*
[(5)] *Takenaka Corporation, suzuki.yousuke@takenaka.co.jp*

Abstract

Much higher level of seismic performance is needed for super-tall buildings due to increased demands for their functional continuities and recognized needs for becoming havens in metropolitan areas. The conventional structural systems can no longer meet the demands, and the vibration control systems using dampers are most commonly used for super-tall buildings in Japan. As the building is taller, however, the dampers are known to deform less, and become less effective at upper stories. This is because the shear drift that produces damper deformation and energy dissipation decreases due to the increased bending (chord) drift at upper stories. The presentation explains this trend, and proposes a simple and reasonably accurate method to predict the shear drift, bending drift, as well as effectiveness of dampers. The method is based on the eigenvalue analysis and static elastic analysis of the member-to-member model of the frame, typically performed during the initial design stage. The method is extended also to formulation of a simplified bending-shear model that accurately simulates the global dynamic behavior of the original model.

The bending stiffness for the bending-shear model is obtained by applying the bending moment at the top of the member-to-member model and obtaining the pure bending deformation. Since the bending moment is constant throughout the building height, the calculation is simple, but calibration to account for some effect of shear force is performed later. Then the contribution from the bending stiffness to the first mode vector of the member-to-member model is estimated and the remaining contribution from the shear stiffness obtained. The procedure in this manner assures that the 1st mode frequency and mode vector of the bending-shear model perfectly match with those of the member-to-member model. We verified the accuracy of this proposed method using 80 and 400m high super-tall buildings with moment frame system, and confirmed remarkable accuracy from the first mode to at least the third mode.

Keywords: Super-tall building; Mass-spring system; Bending-shear model; Vibration period; Mode vector

© The 17th World Conference on Earthquake Engineering

1. Introduction

1.1 Simplified models for analysis of super-tall buildings

Super-tall buildings are increasingly constructed in many metropolitan areas of the world. In order to protect their high socio-economic values, their responses due to earthquakes and/or wind loadings are evaluated carefully by conducting dynamic analyses. Member-to-member (M-) model of the building typically used to check static load effects is not desirable for the dynamic analysis, since it has enormously large degrees-of-freedom (DOF) and requires excessively long computation time.

Overall structural performance and economy of the building must be almost decided during the preliminary design stage. The key parameters for the structural performance would be story-by-story (global) responses such as s shear force, drift angle, acceleration, and ductility factor. The designers, often pressed with time, need to reach satisfactory design by repeating re-analysis and re-design. These necessitate development of a simplified model that simulates the global responses of M-model accurately with much smaller DOF and computation time.

A typical simplified model is a system represented by a mass connected by a bar for each story. The model is divided into two types; the first is shear model where the bar deforms in shear. The second is bending-shear model where the bar deforms in both shear and bending. Limited number of simplified models were proposed in the past [1 - 4], and have been used in Japanese practice while there are limited literatures on their accuracies. More studies are needed on the modeling methods considering a broader range of applicability for various frame types such as moment frame, center core, and outrigger frame, as well as aspect ratio that determines dominance of their shear and bending deformations [5]. The simplified models are also recognized to be useful to determine effectiveness of damper whose action is generated typically by the shear deformation of the frame. The following summarizes the current state of the simplified modeling methods.

1.2 Past modeling methods

Past methods typically consider the results from static analysis applying horizontal story forces to M-model. For the shear model, shear stiffness is directly estimated as shear force divided by the drift at each story. For the bending-shear model, bending deformation is typically evaluated at first. The method by *Muto* et al. [1, 2] is the most common, and it evaluates the bending stiffness and deformation by considering the strain energies caused by axial forces and deformations of all columns of M-model. Subtracting the bending deformation from overall deformation, it obtains shear deformation and corresponding shear stiffness based on the shear force. This method is used in Japanese design guideline [6]. Since it is based on static analysis, its accuracy to simulate dynamic properties of M-model is limited.

The above methods utilizes the output from commercially available seismic analysis software, while the method by *Takabatake* et al. [7, 8] directly models all the members approximately. Since the method assumes locations of inflection points, its error is difficult to grasp. It is more complicated with formulation of various member and joint. The method by *Miranda* [9, 10] connects the two parallel bars deforming in shear and bending, respectively. The method to obtain shear stiffness is not given, and the ratio of shear stiffness to bending stiffness is set constant in throughout the building height. *Lu* [11] applied this method to the simplified analysis of world's second tallest building, Shanghai tower.

1.3 Purpose and structure of this paper

As described above, a simplified model accurately reproducing the dynamic properties of member- to-member (M-) model for super-tall buildings has not been proposed. This paper proposes a new bending-shear model which estimates bending stiffness using the overall deformation of M-model, and does not need to estimate energies of all the members like the previous method [1, 2]. It also accurately reproduces the dynamic properties to higher modes. The accuracy is verified using realistically designed buildings from 60 to 400m tall. This paper, highlights modeling procedures and uses the moment frames only as examples. In the companion paper by *Watai et al.* [12], the method is extended to other structures such as moment frames with center core and/or outrigger frames.

© The 17th World Conference on Earthquake Engineering

2. Previous and proposed simplified models

2.1 Previous models

From static analysis, story displacement u_i and story drift $\Delta u_i = u_i - u_{i-1}$ at i-th story level (i = 1 to n) of the M-model are given. The previous models simulates these static responses.

2.1.1 Previous shear (S-) model

The previous shear (S-) model considers infinite bending stiffness, thus, the shear drift Δu_{si} and stiffness K_{si} are obtained as follows:

$$K_{si} = Q_i / \Delta u_i \tag{1}$$

S-model is accurate for low- to medium-rise buildings (up to about 30-story) having little bending deformation.

2.1.2 Previous bending-shear (B-) model

Previous bending-shear (B-) models are often used for high-rise buildings. The drift Δu_i of M-model is decomposed into bending and shear drifts Δu_{bi} and Δu_{si}, respectively (Fig. 1).

$$\Delta u_i = \Delta u_{bi} + \Delta u_{si} \tag{2}$$

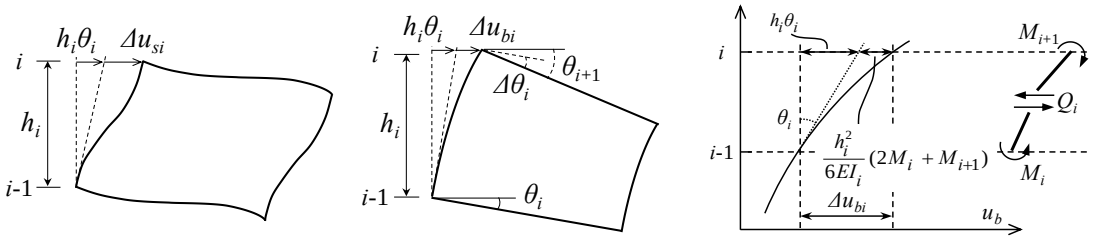

a) Shear drift b) Bending drift c) Bending drift and forces

Fig.1 Conceptual diagram of story drift and its two components

The method evaluates Δu_{bi} and Δu_{si} in order. The well-known method [1, 2] to evaluate Δu_{bi} will be explained. By summing the axial strain energies all of columns from the static analysis of M-model, equivalent incremental rotation angle $\Delta\theta_{ei}$ and corresponding bending stiffness EI_{ei} are obtained as follows:

$$\Delta\theta_{ei} = \sum_{j=1}^{s_i}(N_{ij}\Delta v_{ij}) \Big/ \sum_{j=1}^{s_i}(N_{ij}l_{ij}) \ , \quad EI_{ei} = h_i^2(M_{i+1} + M_i)/2\Delta\theta_{ei} \tag{3a, b}$$

where s_i = number of columns in i-th story, l_{ij} = horizontal distance from the neutral axis to member j, h_i = floor height, and M_i = overturning moment. In equation (3a), the sum of axial strain energies of all columns of M-model is equated with those of a hypothetical case where all the column deformations follow the rotation of flat floor surface like the rotation of plane section of the bar of the B-model.

Using EI_{ei} estimated from equation (3b), Δu_{bi} is obtained based on the beam theory as follows:

$$\Delta u_{bi} = \frac{h_i^2}{6EI_{ei}}(2M_i + M_{i+1}) + h_i \sum_{k=1}^{i-1}\Delta\theta_{ek} \tag{4}$$

Since Δu_i and Δu_{bi} are known, the shear drift Δu_{si} is obtained from equation (2), and the shear stiffness K_{si} is;

$$K_{si} = Q_i / (\Delta u_i - \Delta u_{bi}) \tag{5}$$

© The 17th World Conference on Earthquake Engineering

Accordingly, B-model can be constructed using the values of EI_{ei} and K_{si} obtained from the above procedures. However, the bending drift obtained from the equivalent incremental rotation angle (equation (3a)) does not necessarily assure correct evaluation of the bending drift. One of the reasons is that the work by the overturning moment M_i is not always equal to the axial strain energies of all the columns: its portion becomes energies of local bending of columns and beams which however does not entirely contribute to shear drift.

This kind of problem always exists, whenever drastic reduction of DOF is sought. Extremely large DOF and corresponding energies of the M-model may not be categorized as the two distinct energies of the bending and shear of the B-model. Moreover, the method for the B-model requires enormous calculations scanning through every column. It also does not consider outrigger frames consisting of inclined members and/or core walls not behaving like the column, which are very common to many super-tall buildings.

2.2 Proposed models

The proposed model is formulated to simulate dynamic properties of the super-tall buildings. It exactly simulates the 1st mode circular frequency ω_1 and eigenvector $\boldsymbol{\phi}_1$ of the M-model, where $\boldsymbol{\phi}_1$ = n-DOF horizontal eigenvector representing horizontal displacement of each story, extracted from n_{tot}-DOF of M-model. They are called $S^{(1)}$- and $B^{(1)}$-models in contrast to S- and B-models in Sec. 2.1.

Considering mass matrix **M** with its diagonal term representing horizontal mass m_i of M model, the stiffness matrix **K** of the simplified model must satisfy the following equation;

$$\mathbf{K}\,\boldsymbol{\phi}_1 = \omega_1^2 \mathbf{M}\,\boldsymbol{\phi}_1 \tag{6}$$

The right side of the equation (6) is defined as the 1st mode horizontal force $\mathbf{F^{(1)}}$. Corresponding shear force $Q_i^{(1)}$ and overturning moment $M_i^{(1)}$ are given as follows:

$$Q_i^{(1)} = \sum_{k=i}^{n} F_k^{(1)} = \omega_1^2 \sum_{k=i}^{n} (m_k \phi_{k1}) \quad , \quad M_i^{(1)} = \sum_{k=i}^{n} (Q_k^{(1)} h_k) \tag{7a, b}$$

where ϕ_{i1} = i-th story 1st mode eigenvector. The proposed models are created using $Q_i^{(1)}$ and $M_i^{(1)}$ of M-model.

2.2.1 Proposed shear ($S^{(1)}$-) model

$S^{(1)}$-model assumes that deformation consists of shear drifts only. The shear stiffness K_{si} (i = 1 to n) in **K** of equation (6) is obtained from the following:

$$K_{si} = Q_i^{(1)} \big/ \Delta\phi_{i1} \tag{8}$$

where $\Delta\phi_{i1} = \phi_{i1} - \phi_{i\text{-}1,1}$ = shear drift corresponding to 1st mode eigenvector. Note that a building with a setback configuration may have the 1st mode vector crossing the building neutral position, and it may not be modeled by equation (8), since $Q_i^{(1)}$ and $\Delta\phi_{i1}$ must have the same sign to produce $K_{si} > 0$ at all stories. Except for such a case, the 1st mode properties ω_1 and ϕ_{i1} of $S^{(1)}$-model are identical with those of M-model due to equation (6). Note, however, that ω_j and ϕ_{ij} for the higher modes (j >1) are not always accurate, since the stiffness matrix **K** consists of only the shear stiffness K_{si}'s (i =1 to n) whose values are set by equation (8).

2.2.2 Proposed bending-shear ($B^{(1)}$-) model

As explained in Sec. 2.1, it would be difficult to clearly decompose deformations of the M-model into the two modes of bending and shear. Therefore, instead of the story forces that generate story overturning moments and shear forces simultaneously (Fig. 2a), bending moment M_0 is applied at the top of M-model such that every story is under "pure bending" *i.e.,* constant overturning moment with zero shear (Fig. 2b). Unlike the other method of summing strain energies of all columns, this enables easy and direct estimate for the bending stiffness of the M-model: at story curvature (or rotation increment) p_i at i-th story can be obtained by simply taking the second derivative of displacement u_i, and the bending stiffness $EI_i = M_0 / p_i$ is estimated.

© The 17th World Conference on Earthquake Engineering

Note, however, that this EI_i may need to be adjusted to account for the effect of story shear by the same reason as given in the previous paragraph, and this point will be explained in the later section. Note also that the modeling discussed above clarifies the extent to which a simplified beam theory can reproduce the pure bending deformation of M-model. The locations of load application are shown in Fig. 3, and will be discussed in the later section.

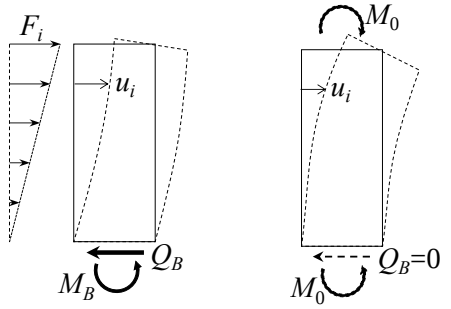

a) Horizontal load (Previous method) b) Pure bending (Proposed method)

Fig.2 Conceptual diagram of static analysis

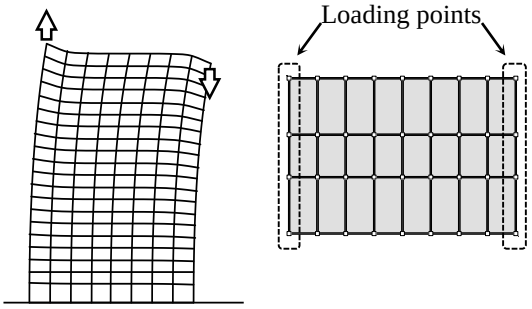

a) Deflection mode b) RFL Plan

Fig.3 Loading method for pure moment

The method involves pure bending analysis of M-model and multiple eigenvalue analyses of $B^{(1)}$-model, respectively. They are explained as follows:

<u>*M-Model Pure Bending Analysis*</u>: The curvature p_i at i-th story, between (i-1)th and i-th levels, is obtained by the following finite difference using the story drift due to pure bending $\Delta u_{bi} = u_{bi} - u_{b,i-1}$:

$$p_i = \left\{ \Delta u_{bi} - (h_i / h_{i-1}) \Delta u_{b,i-1} \right\} / h_i^2 \tag{9}$$

where $h_i = H_i - H_{i-1}$ = floor height, and $u_{b0} = H_0 = \theta_1 = 0$ when calculating for the 1st story. Under pure bending, p_i may differ story-by-story, but it is considered constant within each story.

EI_i of $B^{(1)}$-model is obtained from p_i and adjustment factor α which is 1.0 under pure bending, but is around 0.8 for the buildings considered. Later section explains how to determine α, and

$$EI_i = \alpha M_0 / p_i \tag{10}$$

<u>*$B^{(1)}$-model Eigenvalue analyses*</u>: Using $Q_i^{(1)}$ and $M_i^{(1)}$ of M-model (equation (7)), the 1st mode increment rotation angle $\Delta\theta_{i1}$ and bending drift $\Delta\phi_{bi1}$ of $B^{(1)}$-model are obtained as follows:

$$\Delta\theta_{i1} = \frac{h_i}{2EI_i}(M_i^{(1)} + M_{i+1}^{(1)}), \quad \Delta\phi_{bi1} = \frac{h_i^2}{6EI_i}(2M_i^{(1)} + M_{i+1}^{(1)}) + h_i \sum_{k=1}^{i-1} \Delta\theta_{k1} \tag{11a, b}$$

Since the 1st mode drift $\Delta\phi_{i1} = \phi_{i1} - \phi_{i-1,1}$ of M-model is the constraint and the 1st mode bending drift $\Delta\phi_{bi1}$ of $B^{(1)}$-model is known, shear drift $\Delta\phi_{si1}$ is constrained, and corresponding shear stiffness K_{si} of $B^{(1)}$-model is:

$$K_{si} = Q_i^{(1)} / (\Delta\phi_{i1} - \Delta\phi_{bi1}) \tag{12}$$

From these, the $B^{(1)}$-model having EI_i and K_{si} is created. Note that the model is based on $\Delta\phi_{i1}$, and Eq. 6 is always satisfied. That is, the $B^{(1)}$-model exactly simulates the 1st mode properties of M-model regardless of α-value chosen, thus, α can be used to simulate the 2nd mode properties of M-model. Although α in Eq. 10 is set constant throughout the building height, it has been found very effective: By conducting eigenvalue

© The 17th World Conference on Earthquake Engineering

analysis of B(1) model with initial assumption of α=1, obtained ω_2 and ϕ_2 are compared with those of M-model. Typically, its ω_2 and consequently α need to be lowered. By assuming next α-value, equations (10) to (12) and eigenvalue analyses are repeated until ω_2 and ϕ_2 match well with those of M-model. Typically two to three iterations are enough for coverrgence.

2.3 Relationship between eigenvalue analyses of M-, S(1)-, and B(1)-models

For M-model, consider mass and stiffness matrixes $\mathbf{M_h}$ and $\mathbf{K_{hh}}$ in horizontal DOF and the other residual matrixes $\mathbf{M_r}$, $\mathbf{K_{rr}}$, $\mathbf{K_{hr}}$, and $\mathbf{K_{rh}}$. Likewise, the 1st mode eigenvectors $\boldsymbol{\phi}_{\mathbf{h1}}$ and $\boldsymbol{\phi}_{\mathbf{r1}}$ are defined. The eigenvalue problem for the 1st mode is expressed by:

$$\left\{\begin{bmatrix}\mathbf{K_{hh}} & \mathbf{K_{hr}}\\ \mathbf{K_{rh}} & \mathbf{K_{rr}}\end{bmatrix}-\omega_1^2\begin{bmatrix}\mathbf{M_h} & \mathbf{0}\\ \mathbf{0} & \mathbf{M_r}\end{bmatrix}\right\}\begin{Bmatrix}\boldsymbol{\phi}_{\mathbf{h1}}\\ \boldsymbol{\phi}_{\mathbf{r1}}\end{Bmatrix}=\{\mathbf{0}\} \tag{13}$$

As reasonable approximation, it is assumed $\mathbf{M_h}$ = 0 since the mass in the vertical/rotational direction does not affect the horizontal movement as shown Appendix B. Condensing equation (14),

$$\omega_1^2\mathbf{M_h}\boldsymbol{\phi}_{\mathbf{h1}}=\left[\mathbf{K_{hh}}-\mathbf{K_{hr}}\mathbf{K_{rr}^{-1}}\mathbf{K_{rh}}\right]\boldsymbol{\phi}_{\mathbf{h1}} \tag{14}$$

The vectors on left and right sides of equation (14) are the horizontal force and displacement in the 1st mode. Inside the parentheses on the right side is the dense stiffness matrix obtained from the exact condensation. Note that equation (6) uses the same vectors on the both sides of Eq. 14, thus, S(1)- and B(1)-models exactly reproduce the same 1st mode force and displacement, ω_1 and $\boldsymbol{\phi}_{\mathbf{h1}}$ as in M-model, by using relatively sparse stiffness matrix containing shear stiffness only or combined bending and shear stiffnesses, respectively. However, errors can develop with the other modes due to difference of the stiffness matrixes. While large error is inevitable in S(1)-model, the method proposed in Sec. 2.2.2 appears to minimize the error of B(1)-model for the 2nd mode, by adjusting the balance between its bending and shear stiffnesses.

3. Modeling procedure

In Section 2.2, S(1)- and B(1)-models were proposed. However, since S(1)-model cannot reproduce the higher modal properties of M-model, this paper focuses on B(1) model from now on.

Given ω_1 and ϕ_1, story drift eigenvector $\Delta\phi_{i1} = \phi_{i1} - \phi_{i-1,1}$, as well as the 1st mode overturning moment $M_i^{(1)}$ and shear $Q_i^{(1)}$ of M-model, B(1)-model will be created. The procedure uses M-model analysis in steps 1 to 3, and B(1)-model analysis in steps 4 and 5 as follows:

1) Obtain horizontal displacement u_{bi} due to the bending moment M_0 applied at the top of M-model. As shown by Fig. 3, vertical forces of equal magnitude are applied to all the columns sharing the plane perpendicular to the horizontal force direction, where the plane developing the largest sum of the column axial forces at the 1st story under typical horizontal loading (Fig. 3).
2) Obtain the curvature p_i by using u_{bi} and Eq. 9 where $\Delta u_{bi} = u_{bi} - u_{b,i\text{-}1}$.
3) Obtain bending stiffness EI_i from p_i and adjustment factor α. For the first iteration, α = 1 may be assumed.
4) Obtain the shear stiffness K_{si} using equations (11) and (12).
5) After creating B(1)-model based on steps 3) and 4), conduct its eigenvalue analysis. Confirming the 1st mode properties match with those of M-model, and iterate for the 2nd mode properties by repeating steps 3 to 5 (see the last paragraph of Sec. 2.2.2). Typically, α is reduced until convergence, and it appears to be around 0.8 for the buildings considered in this study. If a negative shear stiffness K_{si} is obtained in this procedure, use the minimum α-value that hold $K_{si} > 0$.

© The 17th World Conference on Earthquake Engineering

4. Overview of example buildings

In this paper, we use two example buildings with a height of 80m (20-story) and 400m (80-story) for demonstrating accuracy of proposed method. Fig. 4 shows the plane and elevation, aspect ratio, natural period of the 1st mode and the ratio to the building height and the period. The members are elastic and X-direction is considered. The 80m model is a 20-story theme structure (trim type) in Reference 6. The 400m model was designed for this study with the members shown Table 1. This model was designed with reference to overseas super-tall buildings and is simplified by removing center core structure, outrigger frame, and seismic studs for our initial study. Note however, that the moment frame structure satisfies the allowable strength against the dead and live loads.

Model		80m	400m
Height	(m)	82.0	400.0
Plan	(m)	51.2 ×35.2	50.0 ×50.0
Aspect ratio	-	1.6	8.0
Story	-	20	80
1st mode natural period	(s)	3.648	8.987
Natural period / Height	(s/m)	0.044	0.022

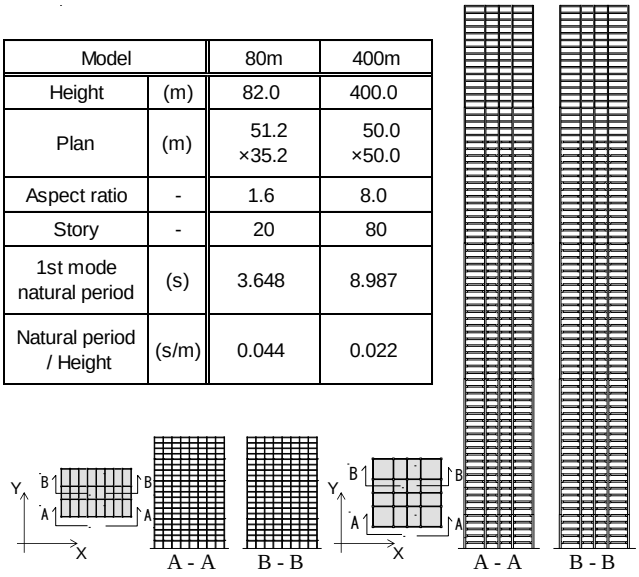

a) 80m model b) 400m model

Fig.4 Building plans and elevations

Table1 Cross section of members (400m model)

Story	Column
66~80F	B□-800×800×40 (SN490)
46~65F	B□-950×950×60 (SA440)
26~45F	B□-1100×1100×60 (SA440), CFT : Fc60
6~25F	B□-1300×1300×80 (SA440), CFT : Fc60
1~5F	B□-1400×1400×80 (SA440), CFT : Fc100

Story	Beam	
	Edge	Center
62~RF	BH-1000×500×19×45 (SM520)	
42~61F	BH-1200×600×24×50 (SM520)	BH-1000×600×24×50 (SM520)
22~41F	BH-1300×700×24×50 (SM520)	BH-1150×700×24×50 (SM520)
2~21F	BH-1400×700×24×50 (SM520)	BH-1150×700×24×50 (SM520)

5. Model accuracies for dynamic properties

This verifies accuracy of S-, B-, and B$^{(1)}$-models for simulating vibration periods and participation. The adjusting factor α = 0.790 and 0.766 for the 80m and 400m models respectively (Chapter 3). The number of DOF of 80m tall M-model is n_{tot} = 980, whereas those of S-, B-, and B$^{(1)}$-models are very reduced and n = 20, 40, and 40, respectively. Similarly, for the 400m tall M-model, n_{tot} = 6865 and those of that of S-, B-, and B$^{(1)}$-models are n = 80, 160, and 160, respectively.

For the 80m and 400m buildings, respectively, Tables 2 and 3 show the 1st to 5th mode vibration periods of M-, S-, B-, and B$^{(1)}$-models and the relative errors of the last three models with respect to M-model. The values exceeding ±3.0% relative error are marked in gray. Figs. 5 and 6 show the participation vector $\beta_j \phi_{ij}$ and corresponding drift vector $\beta_j \Delta \phi_{ij}$.

In the 80m model, the 1st mode vibration periods of S-, B-, and B$^{(1)}$-models match with that of the M-model. B$^{(1)}$-model shows exact match of the first two modes, and the smallest error in the higher modes among the simplified models. S- and B-models show larger errors for the higher mode vibration periods. For example, the error for the 3rd mode is 4.8% and 1.7%, respectively.

Participation vector and corresponding drift of B- and B$^{(1)}$-models almost match with those of M-model, and high accuracy is shown. S-model also seems to show good match with M model when evaluated by participation vector, but corresponding drift of the 3rd mode shows error of about 10% in the upper story.

© The 17th World Conference on Earthquake Engineering

Table2 Comparison of natural periods (80m model)

mode	M model (s)	S model (s)	B model (s)	$B^{(1)}$ model (s)
1	3.648	3.649 (+0.0%)	3.649 (+0.0%)	3.648 (+0.0%)
2	1.357	1.391 (+2.5%)	1.365 (+0.6%)	1.357 (+0.0%)
3	0.811	0.845 (+4.8%)	0.825 (+1.7%)	0.817 (+0.8%)
4	0.576	0.614 (+6.5%)	0.595 (+3.2%)	0.589 (+2.2%)
5	0.436	0.475 (+9.1%)	0.459 (+5.4%)	0.455 (+4.3%)

Note: ■ = error exceeding ±3.0%

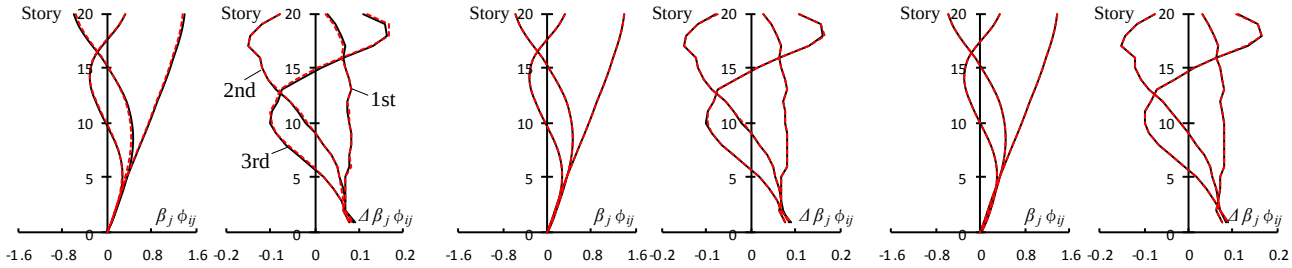

a) S model b) B model c) $B^{(1)}$ model

M model S, B, $B^{(1)}$model

Fig.5 Participation vector of 80m model (Left: displacement Right:Story drift)

In the case of 400m model, the natural periods of first and second modes of $B^{(1)}$ model matched M model, and the relative errors in third, fourth fifth modes were +0.4%, +1.0% and +1.3%. Thus, high modeling accuracy was obtained for first to fifth modes. On the other hand, the relative errors were about 6% in first mode of S and B model. Moreover, the relative error in third mode of S model was as large as +40.4%. The relative error was 0.3% in third mode of B model, but the other mode had a large error. As for the participation vector, $B^{(1)}$ model almost matched M model for first to third mode fairly well. Therefore, $B^{(1)}$ model has high modeling accuracy even for super tall buildings. On the other hand, S model had a large error from M model for first to third modes. B model seemed to show good correspondence with M model, but had a error of about 10% near the top layer. This little error greatly affects the modeling accuracy of natural period and the response to earth quake motion.

Table3 Comparison of natural periods (400m model)

mode	M model (s)	S model (s)	B model (s)	$B^{(1)}$ model (s)
1	8.987	8.448 (-6.0%)	8.371 (-6.8%)	8.987 (+0.0%)
2	2.961	3.614 (+22.1%)	2.886 (-2.6%)	2.961 (+0.0%)
3	1.605	2.253 (+40.4%)	1.610 (+0.3%)	1.612 (+0.4%)
4	1.099	1.616 (+47.0%)	1.118 (+1.7%)	1.110 (+1.0%)
5	0.831	1.284 (+54.5%)	0.854 (+2.7%)	0.842 (+1.3%)

Note: ■ = error exceeding ±3.0%

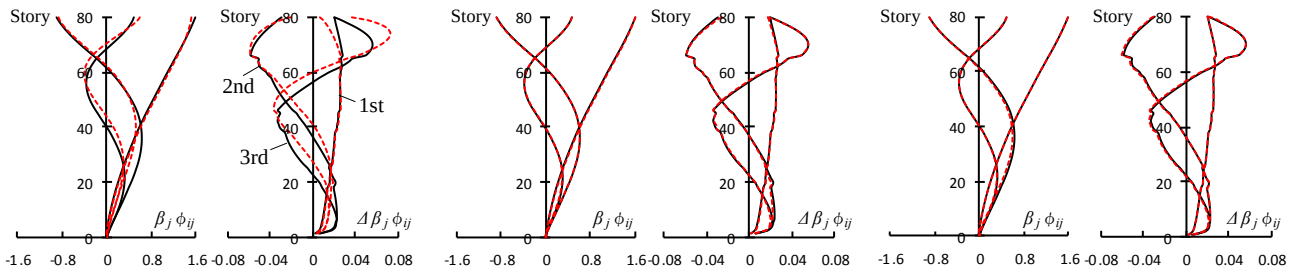

a) S model b) B model c) $B^{(1)}$ model

M model S, B, $B^{(1)}$model

Fig.6 Participation vector of 400m model (Left: displacement Right:Story drift)

© The 17th World Conference on Earthquake Engineering

6. Model accuracies for earthquake responses

In this section, it verifies the accuracy of M, B, $B^{(1)}$ model for seismic response of 400m model. The input ground motion was BCJ-L2 wave, and the structural damping gave Rayleigh damping of $h_1 = h_2 = 0.02$. Figure 7 shows the seismic response spectrum (h = 0.02) and natural periods of B, $B^{(1)}$ model for first mode and natural periods of M model for first to third model.

Figure 8 shows the maximum response values of the absolute acceleration, the displacement, the story drift angle and the shear force when the BCJ-L2 wave input to 400m model. In addition, figure 9 shows the time histories of absolute acceleration of 80th and 40th story. Similarly, figure 10 shows time histories of displacement, figure 11 shows time histories of story drift angle. In these figures, the time of occurring maximum response show as a triangle; A black one (▼) represented M model, a gray one (▼) represented $B^{(1)}$ model and white one (▽) represented B model.

As shown in figure 8, $B^{(1)}$ model had high modeling accuracy because all maximum response values matched M model fairly well. On the other hand, B model shows smaller than M model in displacements and story drift angles. This is because, the displacement response spectrum as shown in figure 7 has tendency to be larger as the natural periods extends. In particular, this is due to the rapid increase in the response value over 8 to 9 second. In the case of super tall building, seismic response value causes a large error with even a slight period shift, since the contribution of the first mode to the displacement response is high. Moreover, the time histories shown in figure 9 to 11, $B^{(1)}$ model reproduced the waveform and the time occurring maximum response of M model fairly well. Although the story drift angle comprise high-order mode components, $B^{(1)}$ model can be accurately reproduced the response of M model because modeling accuracy were good reproduction for high-order mode as shown figure 6. The acceleration response spectrum has a tendency be larger as the short-period components. For the reason, the maximum acceleration response of B model showed a good correspondence. However, the maximum response value occurred time of B model were different from M model and the phase shift became prominently after 40 second. Due to space limitations, only one case is shown in this paper, but it has been confirmed that B(1) model has high modeling accuracy to M model for other ground motions.

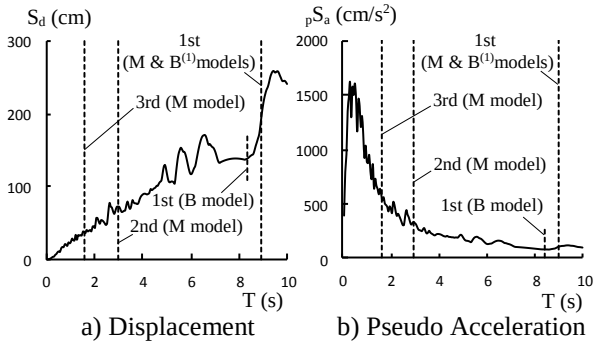

a) Displacement b) Pseudo Acceleration

Fig.7 Response spectrum for BCJ-L2 (h=0.02)

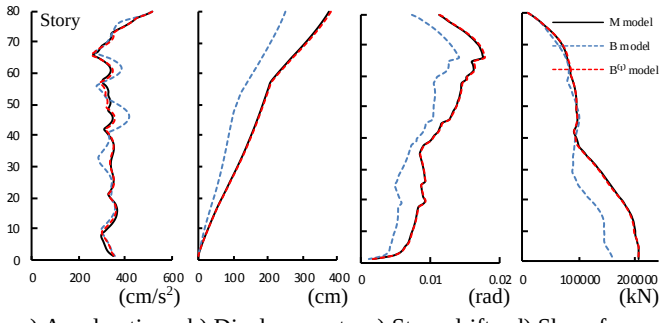

a) Acceleration b) Displacement c) Story drift d) Shear force

Fig.8 Maximum response for BCJ-L2 (400m model)

© The 17th World Conference on Earthquake Engineering

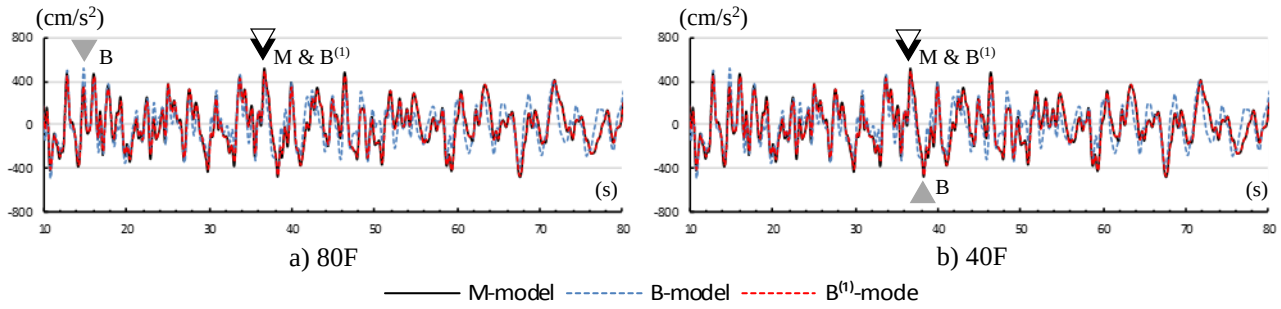

Fig.9 Time history of acceleration for BCJ-L2 (400m model)

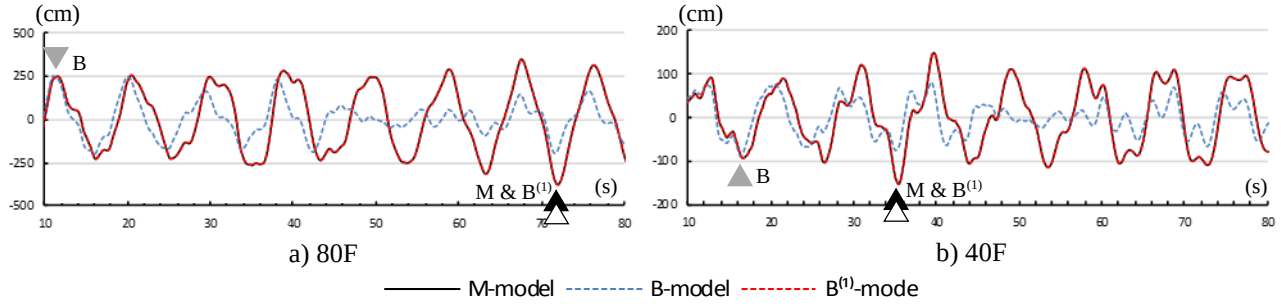

Fig.10 Time history of displacement for BCJ-L2 (400m model)

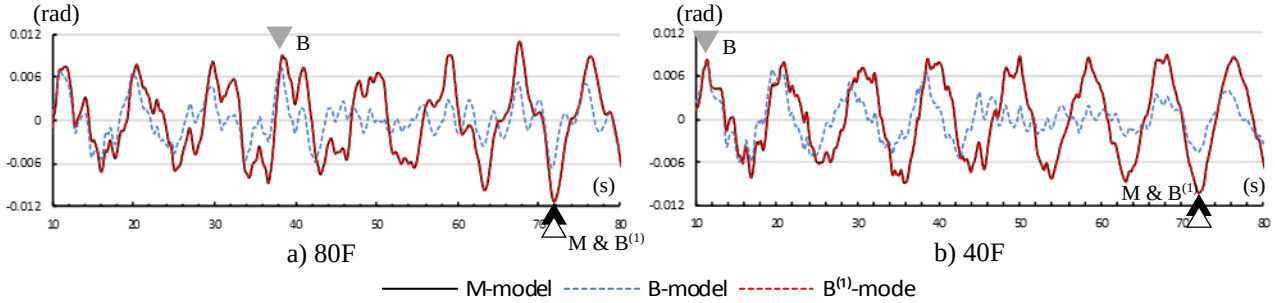

Fig.11 Time history of story drift for BCJ-L2 (400m model)

7. Conclusion

In this paper, it summarized the previous modeling method for mass-spring system, and proposed a new modeling method for bending shear model that can accurately reproduce the dynamic characteristic of building model. In addition, it was shown that this method can be applied 60m to 400m-class super tall buildings with increasing height. These were summarized below.

(1) The mass-spring system constructed with the circular frequency and eigenvector of first mode obtained from the eigenvalue analysis of member-to-member model, can accurately reproduce the dynamic characteristics.

(2) The bending stiffness is can be obtained from only overall response horizontal displacement obtained by pure moment loading analysis without the axial force and deflection of each member were not considered individually unlike the previous method.

(3) The shear / bending stiffness that can accurately reproduce dynamic characteristics to first to third mode of member-to-member model can be obtained by correcting bending stiffness obtained from the pure moment loading analysis.

(4) The bending shear model constructed by proposed method can accurately reproducing the seismic response including the higher-order mode of member-to-member model, while being simple method.

© The 17th World Conference on Earthquake Engineering

8. Acknowledgements

This was a joint research between Tokyo Institute of Technology and Takenaka Corporation, and this work was supported by JST Program on Open Innovation Platform with Enterprises.

9. References

[1] Muto K, Nagata M, Ueno H, Kanayama H, Hanajima M (1979): Earthquake response analysis system of highrise buikding: "FAPP-FASP" system, The 1st Electronic Computer Symposium, 205-210

[2] Osawa Y, Minami T, Matsushima Y, Nagata M (1981): Kenchikugakutaikei38 Kozo no Douteki Kaiseki, SHOKOKUSHA Publishing Co., 222-224

[3] Takahashi M, Fukuzawa E, Isozaki Y (1993): Earthquake response analysis of highrise R/C building in consideration of varying axial force on columns using equivalent vibration model, Journal of structural engineering, Vol.39B, 147-154

[4] Murata M, Nagano M, Hinoura Y, Kitahori T, Tanuma T, Oda S (2019): Statistical analysis of bending deformation components of vibration analysis models and construction of generic bending shear multi-mass models for super high-rise RC buildings, AIJ Technol. Des, Vol.26, No.59, 91-96

[5] M.Nicoreac, J.C.D.Hoenderkamp (2012): Periods of vibration of braced frames with outriggers, Steel Structures and Bridges 2012, Procedia Engineering, Vol.40, 298-303

[6] The Japan Society of Seismic isolation (2013); Manual for Design and Construction of Passively-Controlled Buildings (3rd Edition), 131-152

[7] Takabatake H (1996): A simplified analysis of double symmetric tube structures by the finite difference method, The Structural Design of Tall Buildings, Vol.5(2), 111-128

[8] Takabatake H, Satoh T (2006): A simplified analysis and vibration control to super-high-rise buildings, The Structural Design of Tall and Special Buildings, Vol.15(4), 363-390

[9] Miranda E, Taghavi S (2003); Approximate Floor Acceleration Demands in Multistory Buildings. I: Formulation, Journal of Structural Engineering, Volume 131, Issue 2, 203-211

[10] Taghavi S, Miranda E (2005); Approximate Floor Acceleration Demands in Multistory Buildings. II: Applications, Journal of Structural Engineering, Volume 131, Issue 2, 212-220

[11] Xinzheng L, Linlin X, Cheng Y, Xiao L (2013); Development and application of a simplified model for the design of a super-tall mega-braced frame-core tube building, Engineering Structure, Volume 110, 116-126

[12] Watai K, Kasai K, Maeda S, Sato D, Suzuki Y (2020) ; Application of New Bending-Shear Model for Simplified Analysis of Various Super-tall buildings, 16WCEE, Sendai, JAPAN.

[13] Ishiyama Y (1992): Ai bunpu no tanjou to sono keii, Summaries of Technical Papers of Annual Meeting, Summaries of Technical Papers of Annual Meeting, Architectural Institute of Japan, Structures, 183-184

Appendix A

The building model is represented by a beam. At this time, it is assumed that the bending stiffness EI_i is constant in the layer and the bending moment shits linearly from i-th to (i-1)-th layer. From the basic formula of the beam, the relationship between the horizontal bending displacement u_b of i-th layer, the height H from the ground surface, the shear force Q_i, and the overturning moment M_{i+1} is expressed by the following equation:

$$\frac{d^2u_b}{dH^2} = \frac{1}{EI_i}\left\{M_{i+1} + Q_i\left(H_i - H\right)\right\} \tag{A1}$$

Equation (A1) is solved using the continuous conditions of displacement and rotation angle in i-th and (i-1)-th layer. The increment rotation angle (story rotation angle) $\Delta\theta i$ and story displacement Δu_{bi} are obtained from the following eqations;

© The 17th World Conference on Earthquake Engineering

$$\Delta\theta_i = \frac{h_i}{2EI_i}\left(M_i + M_{i+1}\right) \tag{A2}$$

$$\Delta u_{bi} = \frac{\left(M_i + M_{i+1}\right)h_i^2}{4EI_i} + \frac{Q_i h_i^3}{12EI_i} = \frac{\left(2M_i + M_{i+1}\right)h_i^2}{6EI_i} + h_i \sum_{k=1}^{i-1} \Delta\theta_k \tag{A3}$$

Appendix B

Compare the effective mass ratio between the member-to-member model and mass-spring system. The participation coefficient β_j of j-th mode is defined by equation (A4), and the effective mass ratio $M_{er,j}$ is defined by equation (A5).

$$\beta_j = \boldsymbol{\phi}_j^T \mathbf{M_1} \Big/ \boldsymbol{\phi}_j^T \mathbf{M}\, \boldsymbol{\phi}_j \tag{A4}$$

$$M_{er,j} = \beta_j \boldsymbol{\phi}_j^T \mathbf{M} \beta_j \boldsymbol{\phi}_j \Big/ \sum_{j=1}^{n} \left(\beta_j \boldsymbol{\phi}_j^T \mathbf{M} \beta_j \boldsymbol{\phi}_j\right) \tag{A5}$$

The proposed method is using mass matrix M expressed with only horizontal mass m_i of M model as a diagonal term, however these rations of M model and $B^{(1)}$ model matched as shown table B1. In addition, the relative error of the natural period when the horizontal and vertical mass is given to 400m of M model to the case when the only horizontal mass is given is -0.1%, -0.4%, -0.2%, -0.2% in the first to fifth modes. Similarly, the maximum error of participation vector is very small, that is +0.3%, +0.2%, +0.1%, +0.1%+0.1%. Therefor, the effective of vertical mass is very small for the dynamic characteristics of the building.

Table B1 Effective mass ratio

a) 80m model

mode	M model	S model	B model	$B^{(1)}$ model
1	0.766	0.766	0.766	0.766
2	0.123	0.118	0.122	0.124
3	0.047	0.048	0.047	0.047
4	0.023	0.024	0.023	0.023
5	0.013	0.013	0.012	0.012

b) 400m model

mode	M model	S model	B model	$B^{(1)}$ model
1	0.608	0.623	0.616	0.609
2	0.210	0.156	0.201	0.209
3	0.063	0.063	0.061	0.062
4	0.034	0.037	0.033	0.033
5	0.014	0.021	0.014	0.014

© The 17th World Conference on Earthquake Engineering